Research Square

Preprints are preliminary reports that have not undergone peer review.
They should not be considered conclusive, used to inform clinical practice,
or referenced by the media as validated information.

Integrative Taxonomic and Chemotaxonomic Authentication of Ageratum conyzoides and Conoclinium coelestinum (Asteraceae): The Pharmacological Annotation Diagnostic Key (PADK), a Reproducible Chemotaxonomic Framework

Ozioma Michael
meozioma@delsu.edu.ng

Delta State University
O. M. Agbogidi
Delta State University
A. H. Erhenhi
Delta State University

Research Article

Keywords: integrative taxonomy, species authentication, chemotaxonomy, Ageratum conyzoides, Conoclinium coelestinum, diagnostic key, pharmacological annotation, Asteraceae

Posted Date: August 13th, 2026

DOI: https://doi.org/10.21203/rs.3.rs-10402360/v1

License: This work is licensed under a Creative Commons Attribution 4.0 International License. Read Full License

Additional Declarations: No competing interests reported.

Abstract

Ageratum conyzoides L. and *Conoclinium coelestinum* (L.) DC. are morphologically convergent Asteraceae with overlapping folk-medicinal use across West Africa, and their close resemblance in leaf, root, and inflorescence architecture makes species-level authentication of the medicinal claims attached to each a persistent taxonomic problem. This paper asks whether multiple independent evidence classes can be integrated into a reproducible framework for authenticating such closely related medicinal species, and answers it by constructing the Pharmacological Annotation Diagnostic Key (PADK), an integrative chemotaxonomic authentication framework with pharmacological annotation. Voucher specimens (DELSUH-309, DELSUH-269) from five Delta State localities were authenticated first by gross morphology and developmental anatomy, independently of chemical evidence; volatile chemistry was then profiled by GC-MS (9 compounds in *A. conyzoides*, 22 in *C. coelestinum*) and classified by abundance and distribution; the pharmacological literature for diagnostic markers was then mined under explicit criteria and scored using a mathematically defined Confidence Score and Therapeutic Signature Index. Species identity separated consistently across evidence classes: distinct stem pigmentation and nodal cortex anatomy distinguished the taxa morphologically, while *A. conyzoides* was chemically dominated by α-phellandrene (34.40%) and *C. coelestinum* by fatty-acid methyl esters and phytol. Four independently generated evidence classes — morphology, anatomy, chemotaxonomy, and quantitative phytochemistry — converged on the same species separation; on the independent phytochemical dataset, this separation was further confirmed by leave-one-locality-out cross-validation, which correctly classified all ten held-out samples. Annotated pharmacological profiles — led by anti-inflammatory and antinociceptive activity in *A. conyzoides* and antimicrobial and anti-inflammatory activity in *C. coelestinum* — were concordant with recorded ethnobotanical use and are reported as literature-derived annotations rather than demonstrated properties. PADK demonstrates feasibility on this species pair and is offered as a transferable template for integrative taxonomic authentication of medicinally important, morphologically difficult plant groups, whose broader applicability remains to be tested.

1. INTRODUCTION

Ageratum conyzoides L. and *Conoclinium coelestinum* (L.) DC. are morphologically homologous members of the tribe Eupatorieae (Asteraceae; Patterson and Nesom, 2006) with extensive, overlapping folk-medicinal use across West Africa, yet species-level authentication of the medicinal claims attached to each remains difficult because the two taxa converge strongly in leaf architecture, root habit, and inflorescence structure. A parent taxonomic study resolved this convergence using integrative morphology, developmental anatomy, ecology, phytochemistry, and ethnobotany across five localities in Delta State, Nigeria (Abraka, Agbor, Kwale, Ughelli, and Warri), establishing reliable diagnostic characters at the morphological and anatomical levels. That study also generated a substantial GC-MS dataset describing the volatile chemistry of both species. The present paper addresses a narrower but consequential question: how should that phytochemical dataset be converted into a defensible statement about medicinal relevance, without overstating what GC-MS profiling alone can support?

The central scientific question addressed here is therefore a taxonomic one: can multiple independent evidence classes — morphology, developmental anatomy, volatile chemotype, and quantitative phytochemistry — be integrated into a reproducible framework for authenticating closely related medicinal plant species, in a way that also supports a defensible, non-overstated statement about their medicinal relevance? This premise follows a broader movement toward integrating multiple, independently generated evidence classes in plant taxonomic practice (Maltsev and Erst, 2023). We treat authentication, not pharmacology, as the primary problem, because a dataset containing morphology, anatomy, ecology, phytochemistry, and ethnobotany, but not experimentally generated pharmacological assays, can only support a downstream pharmacological statement that is explicitly bounded as literature-derived annotation rather than demonstrated activity. Rather than asserting that a species is anti-inflammatory or antimicrobial, the framework proposed here states only that, once botanical identity and chemotype have been independently authenticated, a reproducible pathway links that identity to systematically synthesized pharmacological evidence — converting an unfalsifiable efficacy claim into an auditable taxonomic and annotation procedure — in keeping with the broader principle that credible taxonomic identification is a precondition for the conservation, regulation, and medicinal use of plant resources (Heywood, 2007).

The novelty of the approach lies in the pathway rather than in any single component. Conventional volatile-profiling papers follow a short chain: plant → extract → GC-MS → compound list. The framework developed here extends that chain into a decision pathway: plant → taxonomic identity → anatomical confirmation → phytochemical fingerprint → literature-derived pharmacological annotation → diagnostic decision pathway, formalized with explicit equations and tested by internal cross-validation. We term the resulting instrument the Pharmacological Annotation Diagnostic Key (PADK) — an integrative chemotaxonomic authentication framework with pharmacological annotation — and we let the framework's reproducibility and validation results, rather than claims of priority, carry the argument for its usefulness.

Each adjacent single-modality approach addresses part of this problem but not all of it. Morphological keys alone cannot resolve species that converge in leaf, root, and inflorescence architecture, which is precisely the situation motivating this study. Untargeted GC-MS profiling alone produces a compound list but no principled route from that list to a scoped pharmacological statement. DNA barcoding alone authenticates identity but, on its own, carries no chemical or pharmacological information and depends on reference libraries that remain incomplete for many tropical taxa. Classical chemotaxonomic keys authenticate using chemistry but do not, by themselves, formalize how a confirmed marker's presence should be weighted against the pharmacological literature. PADK's contribution is not any one of these steps but the explicit pipeline connecting them, so that a single authenticated specimen carries a traceable path from morphological identity through to a confidence-scored, literature-grounded pharmacological annotation; Table 8 (Section 4.2) sets out this comparison in full once the framework's components have been defined.

The scientific claim of this manuscript is stated plainly: PADK is a reproducible, internally validated framework for integrative taxonomic and chemotaxonomic authentication, with evidence-based pharmacological annotation as its terminal, most tightly bounded application. We do not claim the framework is the first of its kind, or that any individual component — marker classification, literature annotation, confidence weighting — is unprecedented in

isolation; whether the integration of these components is useful and defensible is left for the reader and the data in Sections 3 and 4 to establish. Each adjacent literature (taxonomy, GC-MS profiling, pharmacology, ethnobotany) is drawn upon only insofar as it serves that single, integrative claim.

Section 2 sets out the framework's five phases and the equations that govern them; Section 3 reports the resulting authentication, classification, and internal-validation outcomes; and Section 4 discusses what the framework adds relative to existing approaches, where it can be expected to perform less well, and how it might be extended.

2. MATERIALS AND METHODS

2.1 Study Area and Plant Material

Field material for both species was collected across five ecologically distinct localities in Delta State, Nigeria (Abraka, Agbor, Kwale, Ughelli, and Warri). Voucher specimens were authenticated and deposited at the Delta State University Herbarium (DELSUH) under accession numbers DELSUH-309 (*A. conyzoides*) and DELSUH-269 (*C. coelestinum*). All morphological, anatomical, and phytochemical data used to construct the framework below derive from this authenticated material, previously generated as part of an integrative doctoral taxonomic study (Michael, Agbogidi and Erhenhi, 2026); no new pharmacological assays were performed for the present study.

2.2 Framework Overview

The PADK framework is organized into five sequential phases (Fig. 1): (1) botanical authentication, (2) chemotaxonomic authentication, (3) pharmacological annotation, (4) confidence scoring, and (5) diagnostic key construction. Each phase produces an auditable intermediate output that feeds the next; no phase substitutes literature annotation for experimental proof of bioactivity, and the framework's terminal output is explicitly a diagnostic-annotation instrument rather than an efficacy claim.

2.3 Phase 1: Botanical Authentication Protocol

Species identity was established first and independently of any chemical evidence, following the sequence: species identity → voucher specimen → gross morphology → leaf anatomy → stem anatomy → root anatomy. Qualitative morphological traits (leaf architecture, phyllotaxy, venation, root system, inflorescence structure, stem pigmentation) and quantitative morphometric traits (internodal elongation, root length, petiole length, midrib length, floret counts) were scored across the five localities. Anatomical characters were resolved histologically using safranin–astra-blue differential staining across a 12-week ontogenetic series, tracking nodal cortex configuration, vascular bundle number, cambial activity, trichome density, and lignification pattern. This phase deliberately excludes chemical evidence so that misidentification is ruled out before any chemotaxonomic or pharmacological inference is layered on top.

2.4 Phase 2: Chemotaxonomic Authentication Protocol

Volatile constituents were profiled by GC-MS from chloroform extracts of field-collected foliage. Rather than reporting compounds as an undifferentiated list, each resolved compound was classified along two independent axes. The first axis is abundance-based: primary markers (≥ 15% relative abundance), secondary markers (1–14.9%), accessory markers (< 1%), and absent markers (not detected). The second axis is distributional: diagnostic compounds (differentiate the two species), shared compounds (present in both, informative for genus-level chemotaxonomy), unique compounds (detected in only one species across all sampled localities), population-specific compounds (variable presence across the five localities), and environmental compounds (abundance covarying with site conditions rather than species identity). This dual classification converts a raw chromatogram into taxonomic evidence rather than an inventory.

Each peak's identification confidence was additionally scored from the mass-spectral library search output itself. Peaks for which the top three library-matched candidate structures converged on the same compound class and the same most-probable identity (e.g., α-phellandrene returned consistently as the top hit across replicate library searches) were scored as high-confidence identifications. Peaks for which the top-ranked candidates diverged across structurally distinct compound classes (e.g., a steroid-type versus a heptadienol-type candidate for the same retention time) were scored as tentative identifications and are flagged as such in Table 2. This is a conservative, spectrum-intrinsic confidence indicator; it does not substitute for retention-index co-injection with authentic standards, which we identify as a priority upgrade in Section 4.5.

2.5 Phase 3: Pharmacological Annotation Protocol (Literature Mining)

For every diagnostic, shared, or unique marker identified in Phase 2, a structured, criterion-based literature search was conducted across PubMed, ScienceDirect, and cross-indexed academic search engines, using each compound's IUPAC and common names combined with the terms antimicrobial, anti-inflammatory, antioxidant, antinociceptive, insecticidal, and wound-healing. Searches were conducted between June and July 2026. Inclusion criteria: peer-reviewed primary research or systematic reviews reporting compound-specific (not crude-extract-level) bioactivity, with an identifiable source (journal, year, and, where available, DOI or PubMed ID). Exclusion criteria: sources reporting only extract-level or crude-mixture bioactivity without isolating or synthesizing the specific compound; non-peer-reviewed sources; sources for which the compound identity could not be independently confirmed. The outcomes of this search — records located, records meeting inclusion criteria, the resulting evidence grade, and the pharmacological annotation for each of the seven priority markers — are reported together in Section 3.3, Table 3. This protocol operated at the scale it was actually conducted: a targeted, criterion-based synthesis across seven priority markers, not a full multi-reviewer systematic review with a PRISMA flow diagram (Page et al., 2021) across the entire 31-compound inventory. Extending this protocol to a dual-reviewer systematic review of the complete marker inventory is identified as a specific upgrade path in Section 4.5.

2.6 Phase 4: Confidence Score — Mathematical Definition

The confidence assigned to each compound's pharmacological annotation is computed rather than assigned qualitatively. For compound i, the Confidence Score is:

$$CS_i = W_u \cdot X_u + W_{\square} \cdot X_{\square} + W_r \cdot X_r + W_{\square} \cdot X_{\square} + W_{\square} \cdot X_{\square}$$

where each Xi component is scored on a 1–5 anchored scale and normalized to the unit interval by dividing by 5 before weighting. Uniqueness (X_u) scores distributional exclusivity (5 = detected in only one species across all localities; 1 = detected in both species at comparable abundance). Abundance ($X_{\square}$) scores relative chromatographic abundance in five tiers (1 = < 1%, 2 = 1–4.9%, 3 = 5–14.9%, 4 = 15–24.9%, 5 = ≥ 25%). Replication (X_r) scores the depth of independent literature corroboration (1 = a single primary study, 3 = 4–6 independent studies, 5 = systematic-review-level synthesis across > 15 studies). Breadth ($X_{\square}$) scores the number of independently reported activity categories (1 activity = 1, ≥ 5 concordant activities = 5). Mechanism specificity ($X_{\square}$) scores whether a defined molecular mechanism has been reported (1 = phenomenological report only, 3 = partially characterized, 5 = defined molecular target/pathway, e.g., COX-1/2 or NF-κB modulation). Weights were assigned to prioritize evidentiary strength over chromatographic prominence, reflecting that abundance and distributional uniqueness are chemotaxonomic properties rather than pharmacological evidence: W_u = 0.15, $W_{\square}$ = 0.15, W_r = 0.25, $W_{\square}$ = 0.20, $W_{\square}$ = 0.25 (ΣW = 1.00). CS_i therefore ranges from 0 (no evidentiary support on any criterion) to 1 (maximal support on all five criteria), and is mapped to a five-point scale for reporting: CS ≥ 0.85 = ▣▣▣▣▣; 0.70–0.849 = ▣▣▣▣; 0.55–0.699 = ▣▣▣; 0.40–0.549 = ▣▣; <0.40 = ▣. The equation-derived scores are reported in Table 4 (Section 3.4) and are used, not any earlier qualitative impression, in all downstream calculations including the Therapeutic Signature Index.

A single worked example illustrates the procedure. α-Phellandrene, the highest-scoring compound in Table 4, was rated X_u = 5 (detected only in *A. conyzoides* across all five localities), $X_{\square}$ = 5 (≥ 25% relative chromatographic abundance), X_r = 4 (4–6 independent corroborating studies), $X_{\square}$ = 5 (five concordant reported activities), and $X_{\square}$ = 5 (a defined receptor/pathway target). Normalizing each score to [0,1] and applying the Section 2.6 weights: CS = 0.15(5/5) + 0.15(5/5) + 0.25(4/5) + 0.20(5/5) + 0.25(5/5) = 0.15 + 0.15 + 0.20 + 0.20 + 0.25 = 0.95, mapped to the top tier (▣▣▣▣▣).

Because the weighting scheme (W_u = 0.15, $W_{\square}$ = 0.15, W_r = 0.25, $W_{\square}$ = 0.20, $W_{\square}$ = 0.25) is a design choice rather than an empirically fitted parameter, we tested its influence on the resulting ranking directly rather than asserting robustness. Recomputing CS for all seven Table 4 compounds under an alternative scheme that shifts weight toward chromatographic prominence over evidentiary strength (W_u = 0.30, $W_{\square}$ = 0.10, W_r = 0.20, $W_{\square}$ = 0.20, $W_{\square}$ = 0.20) leaves both extremes of the ranking unchanged: α-phellandrene remains highest (CS 0.95 → 0.96) and α-guaiene remains lowest and in the ▣▣ tier (CS 0.44 → 0.52). The middle of the ranking is more sensitive — phytol, 2,4-di-tert-butylphenol, and hexadecanoic acid methyl ester converge to a three-way tie (CS = 0.86) under the alternative weighting, and two of these compounds move from the ▣▣▣▣ to the ▣▣▣▣▣ tier. The extremes of the confidence ranking, which carry the most interpretive weight in the Discussion and the diagnostic key, are stable to this reweighting, but the tier boundaries in the middle of the distribution are not, and should be read as approximate rather than sharp cutoffs. A full sensitivity sweep across the weight simplex and formal elicitation of the weights from an independent expert panel are natural extensions not attempted here given the scope of a single case-study framework paper (Section 4.5).

2.7 Phase 5: Therapeutic Signature Index — Mathematical Definition

For species s and pharmacological axis a (antimicrobial, anti-inflammatory, antioxidant, antinociceptive/immunomodulatory, insecticidal/nematicide, wound-healing), the raw Therapeutic Signature Index is:

$$TSI_{\square}(s) = \Sigma_i \left[w_{i\square} \times CS_i \times Abund_i(s) \right]$$

summed over all compounds i annotated for axis a in species s, where $w_{i\square} \in \{1.0, 0.5\}$ is the activity-attribution weight (1.0 for a primary reported activity of compound i in the Phase 3 annotation matrix, 0.5 for a secondary or minor reported activity), CS_i is the Phase 4 Confidence Score of compound i, and $Abund_i(s)$ is compound i's relative GC-MS abundance (%) in species s. Raw axis scores are normalized to a common 0–100 scale by dividing every raw value by the single largest raw value observed across the full species × axis matrix and multiplying by 100, so that the single most strongly annotated species-axis combination is fixed at 100 and all other cells are expressed relative to it. Normalized scores are classified as Low (0–25), Moderate (26–50), High (51–75), or Very High (76–100). All raw abundance, weight, and Confidence Score inputs, and the resulting normalized TSI values, are reported in full in Section 3.7 so that the calculation is independently reproducible from the manuscript alone.

Unlike the Confidence Score (Section 2.6), the Therapeutic Signature Index has not itself been subjected to a quantitative robustness check in this manuscript, and we state this limitation explicitly rather than let TSI's validated inputs (CS_i) be read as validating the index itself: CS and TSI answer different questions, and demonstrating the former does not demonstrate the latter. Table 6 (Section 3.7) reports between two and four principal driver compounds per species-axis combination, meaning most TSI values are sums over multiple markers rather than single-compound scores, which limits (but does not eliminate) the influence any one compound's abundance measurement can have on a given axis. A formal leave-one-compound-out sensitivity analysis of TSI would require the complete per-axis $w_{i\square}$ attribution matrix underlying Table 6; we did not tabulate that matrix in the manuscript and so do not report a perturbation analysis we cannot fully reconstruct from the text alone. We flag this as a concrete, well-defined extension for a follow-up validation study, alongside external benchmarking of TSI against an independent bioassay dataset (Section 4.5).

2.8 Internal Validation Protocol

PADK's species-separation claim was tested, not merely asserted, using leave-one-locality-out cross-validation on an independent quantitative dataset: the nine-class quantitative phytochemical composition (alkaloids, steroids, tannins, terpenes, flavonoids, phenols, glycosides, saponins, anthraquinones; mg/100 g) measured for both species at each of the five localities (Abraka, Warri, Ughelli, Agbor, Kwale). This dataset is independent of the GC-MS volatile profile used to build the diagnostic key in Section 3.6, providing a genuine out-of-sample test rather than a circularity check on the same measurements. In each of five folds, one locality's paired samples (one *A. conyzoides*, one *C. coelestinum*) were held out; the remaining four localities' eight samples were z-

standardized (mean and standard deviation computed on the training fold only, to avoid test-set leakage) and used to compute a species centroid in the nine-dimensional standardized feature space; each held-out sample was then assigned to the nearer centroid by Euclidean distance. This procedure was repeated for all five folds (ten held-out classifications in total) and classification accuracy, sensitivity, specificity, precision, and a confusion matrix were computed across all ten out-of-fold predictions (Section 3.5).

The nearest-centroid rule was chosen over more flexible alternatives (linear discriminant analysis, random forest, PLS-DA, or a PCA-reduced classifier) for a dimensionality-driven reason rather than convenience. Each training fold contains eight samples distributed across nine phytochemical-class predictors, so the training sample size does not exceed the number of features (n \u2248 p); in this regime LDA's within-class covariance matrix is singular or near-singular, and both random forest and PCA-based classifiers carry tunable hyperparameters that are prone to overfitting sampling noise rather than the categorical, presence/absence-level separation documented in Section 3.5. The nearest-centroid approach, and its shrunken-centroid extension, is the standard, well-validated choice for exactly this high-dimension, low-sample-size regime in comparable classification settings (Tibshirani et al., 2002), and it has no tunable hyperparameters to overfit within a five-fold validation this small. This reflects a deliberate methodological choice constrained by sample size, not evidence that more elaborate classifiers were unavailable or untried; extending the validation to a larger, independently collected sample (Section 4.3) would be the appropriate setting in which to test whether a more flexible classifier adds discriminative power. PLS-DA in particular is a common alternative in chemotaxonomic classification, but it requires choosing a number of latent components and is well documented to overfit and produce spuriously perfect separation on datasets of this size (single-digit n per class); reporting a PLS-DA result here would have added an appearance of rigor without a genuine increase in evidentiary strength.

2.9 Convergent Multi-Evidence Validation Protocol

As a second, independent line of validation, we tested whether four evidence classes generated by entirely different methods — gross morphology and developmental anatomy (Phase 1), quantitative phytochemistry (Section 2.8), and GC-MS volatile chemotype (Phase 2) — converge on the same species-level separation without being fitted to one another. Concordance across independently collected evidence classes is a standard, low-cost form of validation available whenever multi-modal data already exist, and does not require new laboratory assays (Section 3.8).

3. RESULTS

3.1 Phase 1 — Botanical Authentication

The two species converged strongly on macromorphological traits (simple, ovate, serrated, opposite leaves with reticulate venation; hairy taproot system; corymbose capitula with involucral bracts), consistent with their close phylogenetic affinity. Species-diagnostic separation was instead achieved through stem pigmentation and internal anatomy (Table 1). *A. conyzoides* developed variable reddish- to purplish-brown stem pigmentation at maturity, against consistently green stems in *C. coelestinum*. Nodal cortex configuration diverged developmentally: cross-shaped transitioning to concave in *A. conyzoides*, versus triangulated transitioning to double-convex oblong in *C. coelestinum*. At week 12 of the ontogenetic series, secondary vascular bundle (SVB) counts differed (7 in *A. conyzoides* versus 9 in *C. coelestinum*). Quantitative growth parameters (root length, petiole length, midrib length, floret number) all differed significantly between species by ANOVA (Table 1). This phase rules out misidentification independently of any chemical evidence, and every subsequent phase is conditioned on these authenticated identities.

Table 1
Diagnostic morphological and anatomical characters separating *Ageratum conyzoides* and *Conoclinium coelestinum*, established independently of chemical evidence (Phase 1).

Diagnostic character	***Ageratum conyzoides***	***Conoclinium coelestinum***
Voucher (DELSUH)	DELSUH-309	DELSUH-269
Stem pigmentation	Reddish- to purplish-brown at maturity	Green
Nodal cortex configuration	Cross-shaped → concave	Triangulated → double-convex oblong
SVB count (week 12)	7	9
Root length (ANOVA)	$F(1,8) = 212.761$, $p < 0.001$	(same test, between-species)
Petiole length (ANOVA)	$F(1,8) = 236.977$, $p < 0.001$	(same test, between-species)
Midrib length (ANOVA)	$F(1,8) = 35.459$, $p < 0.001$	(same test, between-species)
Floret number (ANOVA)	$F(1,4) = 26.020$, $p < 0.01$	(same test, between-species)

3.2 Phase 2 — Chemotaxonomic Evidence

GC-MS profiling of chloroform extracts resolved 9 volatile compounds in *A. conyzoides* and 22 in *C. coelestinum*. Classified by relative abundance, *A. conyzoides* carried two primary markers (≥ 15%: α-phellandrene, 34.40%; α-guaiene, an azulene-type sesquiterpene, 27.31%) and six secondary markers (1–14.9%), with no marker falling below 1%. *C. coelestinum* carried four primary markers (9,12-octadecadienoic acid methyl ester, 25.88%; hexadecanoic acid methyl ester, 24.59%; phytol, 17.43%; 9,12,15-octadecatrienoic acid methyl ester, 15.33%), three secondary markers, and eighteen accessory markers (< 1%), predominantly branched-chain fatty-acid methyl esters. Classified by distribution, phytol was the only marker detected in both species — present as a secondary marker in *A. conyzoides* (2.88%) and as a primary marker in *C. coelestinum* (17.43%) — and is therefore treated as a shared, abundance-diagnostic marker. Every other primary or secondary marker in each species' profile was detected exclusively in that species across all five localities and is therefore

treated as a unique marker (Table 2). Applying the identification-confidence criterion of Section 2.4, five of the seven priority markers returned a single, class-consistent top library match across candidate structures (high identification confidence); α-guaiene and 3,5-heptadien-2-ol/steroid-type peaks returned structurally divergent top candidates (tentative identification), flagged accordingly in Table 2. No marker showed a distribution pattern attributable to site rather than species identity within the primary/secondary tier, though several accessory markers in *C. coelestinum* varied in trace abundance across localities, consistent with population-specific or environmentally modulated expression.

Table 2
Primary, secondary, and diagnostic-accessory volatile markers classified by relative abundance, cross-species distribution, and spectral identification confidence (Phase 2; Section 2.4). Full 31-compound inventory (9 + 22 compounds) available on request.

Compound	Species	Rel. abundance	Abundance tier	Distribution class	ID confidence
α-Phellandrene	*A. conyzoides*	34.40%	Primary	Unique	High
α-Guaiene (azulene-type sesquiterpene)	*A. conyzoides*	27.31%	Primary	Unique	Tentative
Aromandendrene / caryophyllene-type sesquiterpene	*A. conyzoides*	9.58%	Secondary	Unique	High
2,4-Di-tert-butylphenol	*A. conyzoides*	4.79%	Secondary	Unique	High
Phytol	*A. conyzoides*	2.88%	Secondary	Shared (abundance-diagnostic)	High
9,12-Octadecadienoic acid, methyl ester	*C. coelestinum*	25.88%	Primary	Unique	High
Hexadecanoic acid, methyl ester	*C. coelestinum*	24.59%	Primary	Unique	High
Phytol	*C. coelestinum*	17.43%	Primary	Shared (abundance-diagnostic)	High
9,12,15-Octadecatrienoic acid, methyl ester	*C. coelestinum*	15.33%	Primary	Unique	High
Methyl stearate	*C. coelestinum*	5.51%	Secondary	Unique	High
Neophytadiene	*C. coelestinum*	4.45%	Secondary	Unique	Tentative
Santolina triene	*C. coelestinum*	0.63%	Accessory	Unique (trace diagnostic)	High

3.3 Phase 3 — Pharmacological Annotation Matrix

Applying the literature-mining protocol (Section 2.5) to the seven priority markers produced both the search outcomes and the resulting pharmacological annotation, consolidated in Table 3. Five markers (phytol, 2,4-di-tert-butylphenol, α-phellandrene, hexadecanoic acid methyl ester, and the combined linoleate/linolenate esters) returned at least one compound-specific primary or review-level source meeting inclusion criteria, graded Moderate to High evidence. Neophytadiene returned a single compound-specific in vivo source (Moderate evidence). α-Guaiene returned only class-level azulene/guaiane annotation, with no compound-specific bioassay located, and is graded Low evidence — a result carried forward explicitly into its Confidence Score (Section 3.4). Phytol returned the broadest and most mechanistically characterized annotation: an acyclic diterpene alcohol with repeatedly documented antimicrobial, anti-inflammatory, antioxidant, antinociceptive, and immune-modulating effects, with in vivo work implicating cyclooxygenase (COX-1/2) and NF-κB pathway modulation (Islam et al., 2018). 2,4-Di-tert-butylphenol, unique to *A. conyzoides*, is repeatedly reported as a potent antimicrobial phenolic with minimum inhibitory concentrations in the low-μg/mL range against multidrug-resistant Gram-positive pathogens, alongside antioxidant and biofilm-inhibitory activity (Sundar and Arunachalam, 2025). α-Phellandrene, the dominant primary marker of *A. conyzoides*, has the most mechanistically resolved antinociceptive annotation of any compound in the matrix, with evidence implicating glutamatergic, opioid, nitrergic, cholinergic, and adrenergic pathways, alongside neutrophil-migration-dependent and tissue-protective anti-inflammatory activity (Lima et al., 2012; Siqueira et al., 2016; Gonçalves et al., 2020). Hexadecanoic acid methyl ester, the dominant fatty-acid ester of *C. coelestinum*, carries consistent antimicrobial, antioxidant, nematicide, and hypocholesterolemic annotation across multiple independent GC-MS bioprospecting studies, including a direct antibacterial demonstration against multidrug-resistant clinical isolates (Shaaban et al., 2021). The co-dominant unsaturated esters 9,12-octadecadienoic acid methyl ester (methyl linoleate) and 9,12,15-octadecatrienoic acid methyl ester (methyl linolenate) are recurrently co-annotated with anti-inflammatory, hepatoprotective, and antimicrobial activity in comparable volatile-profiling literature. Neophytadiene, a secondary marker in *C. coelestinum*, is annotated with antimicrobial and CNS-modulating (anxiolytic-like) activity in in vivo neuropharmacological screening.

Table 3

Literature-mining search outcomes and pharmacological annotation matrix for the seven priority chemotaxonomic markers (Phase 3; Section 2.5). Annotatio reflects literature-reported bioactivity of the authenticated compound; it is not an experimental measurement in *A. conyzoides* or *C. coelestinum* extracts. α-Guaiene's Low evidence grade despite high chromatographic abundance is carried forward explicitly into its Confidence Score (Section 3.4).

Compound	Species (this study)	Search outcome (located → retained)	Evidence grade	Reported activity	Mechanism / evidence level	Corroboration depth
Phytol	*Both (secondary in A. conyzoides; primary in C. coelestinum)*	1 systematic review (> 100 studies) + 1 mechanistic study retained	High	Antimicrobial, anti-inflammatory, antioxidant, antinociceptive, immunomodulating	COX-1/2 & NF-κB modulation; membrane interaction — in vitro + in vivo	Extensive (systematic review synthesizing > 100 primary studies)
2,4-Di-tert-butylphenol	*A. conyzoides (unique)*	4 located, 2 retained	Moderate–High	Antimicrobial (incl. MRSA/VRE), antioxidant, antibiofilm, anticancer (in vitro)	Membrane/biofilm disruption; free-radical scavenging — in vitro	Multiple independent isolations (Streptomyces, Fusarium, algal, plant sources)
α-Phellandrene	*A. conyzoides (unique, primary)*	5 located, 3 retained	High	Antinociceptive, anti-inflammatory, immunomodulatory, wound-healing, antimicrobial	Glutamatergic/opioid/nitrergic/cholinergic pathways; neutrophil-migration inhibition — in vivo	Multiple (Lima et al. 2012 and citing literature)
Hexadecanoic acid, methyl ester	*C. coelestinum (unique, primary)*	3 located, 2 retained (1 direct antibacterial demonstration)	Moderate–High	Antimicrobial, antioxidant, nematicide, insecticide, hypocholesterolemic	Membrane-level antibacterial action — in vitro	Multiple independent GC-MS bioprospecting reports
Methyl linoleate / linolenate esters	*C. coelestinum (unique, primary)*	Recurrent co-annotation; 1 class-level source retained (no compound-isolated mechanistic study)	Moderate	Anti-inflammatory, hepatoprotective, antiacne, antiproliferative, antimicrobial	Cytokine modulation — in vitro/in vivo (extract-associated); recurrent co-annotation	Moderate, recurrent across volatile-profiling literature
Neophytadiene	*C. coelestinum (unique, secondary)*	2 located, 1 retained	Moderate	Antimicrobial, anxiolytic/sedative (CNS)	Gram-positive/negative and fungal inhibition; GABAergic modulation — in vivo	Moderate
α-Guaiene	*A. conyzoides (unique, primary)*	0 compound-specific sources retained (class-level azulene/guaiane annotation only)	Low — class-level inference only	Anti-inflammatory (class-level azulene/guaiane annotation only)	Not compound-specifically resolved — low specificity	Sparse / class-level inference only

3.4 Phase 4 — Confidence Scoring

Applying the Confidence Score equation (Section 2.6, CS = W_uX_u + W□X□ + W_rX_r + W□X□ + W□X□) to the seven priority markers produced the values in Table 4. α-Phellandrene returned the highest score (CS = 0.95, □□□□□), driven by maximal scores on uniqueness, abundance, breadth, and mechanism specificity. Phytol followed closely (CS = 0.91, □□□□□) despite a reduced uniqueness component (X_u = 3/5, reflecting its shared rather than exclusive distribution), because its replication, breadth, and mechanism scores are all maximal. 2,4-Di-tert-butylphenol and hexadecanoic acid methyl ester both scored CS = 0.82 (□□□□): high on uniqueness and breadth, but capped by comparatively modest abundance (2,4-DTBP) or mechanism-specificity (hexadecanoic acid methyl ester, for which antibacterial action has been demonstrated but not deeply mechanistically resolved). The combined methyl linoleate/linolenate esters scored CS = 0.73 (□□□□). Neophytadiene scored CS = 0.59 (□□□). α-Guaiene, despite the highest possible uniqueness and abundance scores (27.31% relative abundance, detected in no other marker set), scored only CS = 0.44 (□□), because its replication, breadth, and mechanism-specificity components were all minimal (Table 3) — the equation-derived result confirms, quantitatively, that chromatographic prominence alone does not generate pharmacological confidence.

Table 4
Confidence Score components and computed values (Phase 4; Section 2.6). CS = $0.15X_u + 0.15X_a + 0.25X_r + 0.20X_b + 0.25X_m$, each Xi normalized to [0,1] before weighting.

Compound	X_u (Uniq.)	X_a (Abund.)	X_r (Replic.)	X_b (Breadth)	X_m (Mechanism)	CS	Stars
Phytol	3/5	4/5	5/5	5/5	5/5	0.91	★★★★★
α-Phellandrene	5/5	5/5	4/5	5/5	5/5	0.95	★★★★★
2,4-Di-tert-butylphenol	5/5	2/5	4/5	4/5	5/5	0.82	★★★★
Hexadecanoic acid, methyl ester	5/5	4/5	4/5	5/5	3/5	0.82	★★★★
Methyl linoleate / linolenate esters	5/5	4/5	3/5	4/5	3/5	0.73	★★★★
Neophytadiene	5/5	2/5	3/5	2/5	3/5	0.59	★★★
α-Guaiene	5/5	5/5	1/5	1/5	1/5	0.44	★★

3.5 Internal Validation: Leave-One-Locality-Out Classification

Applying the leave-one-locality-out protocol (Section 2.8) to the independent nine-class quantitative phytochemical dataset (alkaloids, steroids, tannins, terpenes, flavonoids, phenols, glycosides, saponins, anthraquinones; original source data reported per locality in the parent thesis dataset), all ten held-out samples (one *A. conyzoides* and one *C. coelestinum* sample from each of the five localities, predicted from a centroid trained on the remaining four localities in each fold) were correctly classified (accuracy = 10/10 = 100%; Table 5, Fig. 2). Sensitivity (correct recall of *A. conyzoides*) and specificity (correct recall of *C. coelestinum*) were both 100%, as was precision. The nearest-centroid distances (Table 5) show a wide margin between the correct- and incorrect-class distances in every fold (minimum margin = 1.86 standardized units, Ughelli *C. coelestinum* fold), indicating the separation is not a borderline result. This margin reflects a real biological pattern rather than a statistical artefact of a small sample: steroids, tannins, flavonoids, and anthraquinones were categorically absent (0.00 mg/100 g) in every *A. conyzoides* sample across all five localities and present in every *C. coelestinum* sample, while terpenes showed the reverse pattern (present at 13.6–23.4 mg/100 g in *A. conyzoides*, absent or trace in *C. coelestinum*). Stated plainly: with a categorical, presence/absence-level separation of this kind, a simple threshold rule would achieve the same 100% accuracy, and the leave-one-locality-out result should be read as confirming that this categorical separation is stable across all five sampled localities, not as a demonstration that PADK can resolve harder cases where candidate species share a similar phytochemical class profile. That is a distinct and unresolved question, addressed in Section 4.3.

Table 5
Leave-one-locality-out classification results across all five folds (10 held-out samples). Distances are standardized (z-scored on training fold) Euclidean distances to each species centroid; the sample is assigned to the nearer centroid.

Held-out locality	True species	Predicted species	Distance to A.c. centroid	Distance to C.c. centroid	Correct?
Abraka	*A. conyzoides*	*A. conyzoides*	0.95	4.76	Yes
Abraka	*C. coelestinum*	*C. coelestinum*	5.10	1.03	Yes
Warri	*A. conyzoides*	*A. conyzoides*	0.84	5.34	Yes
Warri	*C. coelestinum*	*C. coelestinum*	7.73	5.90	Yes
Ughelli	*A. conyzoides*	*A. conyzoides*	1.80	4.87	Yes
Ughelli	*C. coelestinum*	*C. coelestinum*	5.62	2.32	Yes
Agbor	*A. conyzoides*	*A. conyzoides*	0.92	5.22	Yes
Agbor	*C. coelestinum*	*C. coelestinum*	4.82	1.04	Yes
Kwale	*A. conyzoides*	*A. conyzoides*	0.83	5.19	Yes
Kwale	*C. coelestinum*	*C. coelestinum*	5.28	2.03	Yes

3.6 Phase 5 — The Pharmacological Diagnostic Key

The confidence-scored annotations were compiled into a dichotomous diagnostic key routing a sample from raw chemotype markers to a species-level call and an associated predicted pharmacological signature (Fig. 3). The key operates on two concordant marker checks. First-level separation distinguishes a monoterpene/sesquiterpene-dominated profile (α-phellandrene > 30% relative abundance, with 2,4-di-tert-butylphenol present) from a fatty-acid-methyl-ester-dominated profile (hexadecanoic acid and 9,12-octadecadienoic acid methyl esters jointly exceeding 45%). Second-level confirmation cross-checks a second, independent marker together with the Phase 1 morphological character (stem pigmentation) already established without reference to chemistry: an azulene-type sesquiterpene marker (α-guaiene) exceeding 25%, co-occurring with reddish-to-purplish-brown stem pigmentation, confirms an *A. conyzoides* chemotype; phytol exceeding 15% co-occurring with trace Santolina triene and green stem pigmentation confirms a *C. coelestinum* chemotype. Assignment confidence scales with the number of concordant markers recovered: a single matching marker yields a provisional call, while three or more concordant markers yield a high-confidence call. Each terminal node carries a predicted pharmacological signature (antinociceptive/anti-inflammatory-leaning for *A. conyzoides*; antimicrobial/antioxidant-leaning for *C. coelestinum*) that is explicitly a literature-derived annotation, not an experimentally confirmed species

property. Unlike the volatile-marker thresholds in this key, which have not yet been tested against out-of-sample chromatograms, the underlying species separation itself was tested directly using the independent phytochemical-class dataset in Section 3.5, where it achieved 100% out-of-sample accuracy.

3.7 Therapeutic Signature Index

Applying the TSI equation (Section 2.7) across the six pharmacological axes and both species produced the normalized 0–100 index in Table 6 and Fig. 4. *C. coelestinum*'s profile is anchored by a Very High antimicrobial score (TSI = 100.0, the matrix maximum, driven jointly by hexadecanoic acid methyl ester, the linoleate/linolenate esters, phytol, and neophytadiene) and a Very High anti-inflammatory score (TSI = 85.6, driven by the high-abundance methyl esters and phytol). *A. conyzoides*'s profile is anchored by a Very High anti-inflammatory score (TSI = 76.9) and a High antinociceptive/immunomodulatory score (TSI = 65.7), both driven overwhelmingly by α-phellandrene's high abundance (34.40%) and high Confidence Score (0.95). *A. conyzoides* scored Low on the antioxidant (12.2) and insecticidal/nematicide (0.0) axes: no marker in its confidence-scored annotation matrix carries a primary literature-reported antioxidant or insecticidal activity, so the equation correctly returns a floor value rather than inferring an unsupported activity. This is a substantive finding, not a gap in the analysis: the TSI's zero and near-zero values are as informative as its high values, because they show the equation is not defaulting to a favorable score in the absence of evidence.

Table 6
Therapeutic Signature Index (TSI, 0–100, normalized to matrix maximum) by pharmacological axis, with classification bins (Low 0–25, Moderate 26–50, High 51–75, Very High 76–100) and principal literature-annotated driver compound(s) per species.

Pharmacological axis	*A. conyzoides* TSI	Class	*C. coelestinum* TSI	Class	Principal driver compound(s)
Antimicrobial	42.6	Moderate	100.0	Very High	2,4-DTBP+Phytol / Hexadecanoic ME+esters+Phytol+Neophytadiene
Anti-inflammatory	76.9	Very High	85.6	Very High	α-Phellandrene+Phytol + α-Guaiene / Linoleate–linolenate esters+Phytol
Antioxidant	12.2	Low	67.1	High	2,4-DTBP+Phytol / Hexadecanoic ME+Phytol
Antinociceptive / immunomodulatory	65.7	High	32.0	Moderate	α-Phellandrene+Phytol / Phytol+Neophytadiene
Insecticidal / nematicide	0.0	Low	37.6	Moderate	(none annotated) / Hexadecanoic acid ME
Wound-healing	35.3	Moderate	29.5	Moderate	α-Phellandrene+Phytol / Phytol

3.8 Convergent Multi-Evidence Validation

Four evidence classes, generated by four methodologically independent procedures, were tested for whether they converge on the same species-level separation without being fitted to one another (Table 7). Gross morphology and developmental anatomy (Phase 1) separated the species on stem pigmentation, nodal cortex configuration, and four significant ANOVA comparisons (root, petiole, and midrib length; floret number). Quantitative phytochemistry (Section 2.8) separated the species categorically on five of nine chemical classes (steroids, tannins, flavonoids, and anthraquinones present only in *C. coelestinum*; terpenes present almost exclusively in *A. conyzoides*) across all five localities, and this separation alone achieved 100% leave-one-locality-out classification accuracy (Section 3.5). GC-MS volatile chemotype (Phase 2) separated the species on entirely non-overlapping primary marker sets (α-phellandrene/α-guaiene versus fatty-acid methyl esters), with only phytol shared, at a five-fold higher relative abundance in *C. coelestinum*. All three evidence classes were generated from different plant tissues, different analytical instruments, and different statistical procedures, yet none produced an ambiguous or contradictory species call at any of the five localities. This convergence is the strongest single piece of validation evidence in the manuscript, precisely because none of the three methods was designed with reference to the others.

Table 7
Convergent multi-evidence validation: three independently generated evidence classes separate the two species identically across all five sampled localities (Section 2.9, Section 3.8).

Evidence class	Method	Basis of species separation	Concordant with GC-MS chemotype?
Morphology & anatomy	Histological staining, morphometry, ANOVA (Phase 1)	Stem pigmentation; nodal cortex configuration; 4 significant ANOVA traits	Yes — 100% (5/5 localities)
Quantitative phytochemistry	Standard phytochemical class assay (mg/100 g), 9 classes × 5 localities	Categorical presence/absence of steroids, tannins, flavonoids, anthraquinones, terpenes	Yes — 100% (5/5 localities; leave-one-out accuracy 100%)
GC-MS volatile chemotype	Chloroform extraction + GC-MS (Phase 2)	Non-overlapping primary marker sets; shared marker (phytol) at divergent abundance	— (reference class)

3.9 Concordance with Ethnobotanical Use Patterns

Ethnobotanical surveys across the same five localities recorded use of both species for eye conditions, fever, stomach pain, infections, and intoxication, prepared as leaf/flower decoctions for bathing or drinking, or as chewed flowers to counteract poison; *A. conyzoides* additionally carried ritual and spiritual-protection uses ('gun medicine') not reducible to a pharmacological axis. The infection- and fever-related folk uses recorded for both species are broadly concordant with the antimicrobial annotation recovered independently for both chemotypes (2,4-DTBP-driven in *A. conyzoides*; hexadecanoic acid methyl ester- and phytol-driven in *C. coelestinum*), and the stomach-pain/analgesic-adjacent uses are concordant with the antinociceptive annotation led by α-phellandrene in *A. conyzoides*. This concordance is presented as corroborating context, not as validation in the statistical sense used in Sections 3.5 and 3.8:

folk use documents traditional recognition of bioactivity, while the annotation matrix documents literature-reported bioactivity of the isolated compound; neither substitutes for the extract- or compound-level bioassay that would be required to close the inferential loop.

4. DISCUSSION

4.1 Authentication First: Bounding the Pharmacological Annotation

A predictable question follows from a framework that links authenticated botanical identity to evidence-based pharmacological annotation: why attach any pharmacological language at all to a dataset containing no original bioassay? The framework does not infer biological activity from GC-MS data alone, and pharmacology is deliberately the last, most tightly bounded step in the pipeline, conditioned on morphological, anatomical, and chemotaxonomic authentication that precedes it. Pharmacological attributes were assigned only where supported by peer-reviewed evidence for the authenticated compound itself, following a documented literature-mining protocol (Section 2.5, Table 3) and a mathematically defined confidence score (Section 2.6, Table 4). The framework is an annotation system rather than an efficacy assessment. Every table in this manuscript that reports a pharmacological property reports it as a property of the compound in the cited external literature, cross-referenced against the compound's confirmed presence and abundance in an authenticated species — not as a property measured in that species by this study. This distinction, and the equations in Sections 2.6–2.7 that operationalize it, is the load-bearing methodological claim of the paper.

4.2 Comparison with Conventional Approaches

Table 8 summarizes PADK's position relative to six adjacent traditions; three distinctions are worth stating in prose. Against conventional descriptive GC-MS reporting — a compound list glossed with unweighted, uncited, or extract-level bioactivity claims — PADK adds an explicit inclusion protocol (Table 3), a mathematically reproducible confidence score (Section 2.6), and a tested rather than asserted species-separation claim (Section 3.5). Against classical morphology-based chemotaxonomic keys (Simpson, 2010), PADK does not replace morphological diagnosis — Phase 1 is retained as the taxonomic foundation and remains the highest-confidence, lowest-cost evidence class — but adds a pharmacologically interpretable second layer on top of it. And against formal evidence-synthesis methodology (GRADE, PRISMA), PADK's literature protocol (Table 3) borrows the vocabulary of inclusion criteria and evidence grading but does not meet the bar of a registered, dual-reviewer systematic review, a limitation stated explicitly in Section 2.5. Against DNA barcoding, the molecular alternative for species-level authentication, PADK trades sequence-level resolution for accessibility: barcoding requires curated reference libraries that remain sparse for many tropical Asteraceae and is not itself a source of pharmacological information, whereas Phase 1's morphological and anatomical characters (Table 1) are field-diagnosable without laboratory sequencing capacity, consistent with recent syntheses of the practical constraints on barcode-based authentication in under-referenced floras (Zhu et al., 2022). More broadly, PADK sits within a wider push to combine chemical, morphological, and molecular evidence for medicinal-plant authentication rather than relying on any single modality (Amin and Park, 2025).

4.3 Where the Framework Will Fail

PADK's demonstrated performance in this manuscript rests on a case that is favorable to it in several specific ways, and the framework should be expected to perform less well outside those conditions. First, and most directly, the leave-one-locality-out validation in Section 3.5 classified ten held-out samples; a 100% accuracy figure on a sample of that size is a promising internal-consistency check, not evidence of generalization, and should be read as such until tested on independently collected, larger samples. Second, *A. conyzoides* and *C. coelestinum* happen to diverge categorically, not just quantitatively, on several phytochemical classes; congeneric pairs with more gradual, quantitative-only divergence — arguably more taxonomically interesting than the present case — would likely classify less cleanly under the same protocol, and PADK provides no mechanism for estimating that accuracy in advance. Third, the diagnostic key's volatile-marker thresholds (Section 3.6, Fig. 3) were set by inspection of the present dataset and have not themselves been cross-validated; a threshold tuned to one dataset risks overfitting when applied to independently collected chromatograms, given the known sensitivity of monoterpene ratios to extraction method, plant age, and season. Fourth, the Confidence Score and Therapeutic Signature Index are only as good as the underlying literature search (Section 2.5), and the entire pharmacological annotation layer inherits whatever publication bias exists in that literature; the Replication and Mechanism-specificity criteria in the Confidence Score (Section 2.6) partially, but do not fully, correct for this.

4.4 Where the Framework Can Be Generalized

The five-phase structure (botanical authentication → chemotaxonomic classification → literature annotation → mathematical confidence scoring → diagnostic key/index construction) does not depend on any feature specific to Asteraceae, to volatile chemistry, or to the two species studied here. It is directly transferable to any pair or small set of taxonomically difficult medicinal taxa for which (i) at least one objective, chemistry-independent diagnostic character exists for Phase 1, (ii) a compound-level chemical profile (GC-MS, LC-MS, HPLC, or comparable) is available for Phase 2, and (iii) a peer-reviewed pharmacological literature exists for at least some resolved compounds for Phase 3. Where multiple independently generated evidence classes already exist for the taxa in question — as they did here, in the form of the pre-existing quantitative phytochemistry dataset used for Section 3.5's validation — the convergent multi-evidence check of Section 3.8 is essentially free to add and substantially strengthens the framework's evidentiary standing without new laboratory work. This is a common circumstance in tropical ethnobotanical research, where multi-modal, thesis-scale datasets are frequently collected but rarely cross-validated against one another.

4.5 Limitations and Upgrade Path

Two further limitations, distinct from the failure modes discussed in Section 4.3, define a concrete upgrade path. First, the GC-MS dataset was generated from a single extraction solvent (chloroform) at a single developmental stage, without retention-index co-injection against authentic standards; the identification-confidence flag introduced in Section 2.4 is a partial, spectrum-intrinsic safeguard, not a substitute for the standard co-injection protocols expected for reliable compound-level measurement in natural products chemistry (Betz et al., 2011), which we identify as the highest-priority analytical

upgrade. Second, the literature-mining protocol (Section 2.5, Table 3) is a targeted, criterion-based synthesis across seven priority markers conducted by a single reviewer, not a registered, dual-reviewer PRISMA-compliant systematic review across the full 31-compound inventory; extending it to that standard is a defined, tractable next step rather than a structural limitation of the framework itself.

4.6 Testable Hypotheses for Experimental Validation

The confidence-ranked annotation matrix (Table 4) generates a falsifiable set of experimental hypotheses, prioritized by Confidence Score, that would close the inferential loop this manuscript deliberately leaves open. For *A. conyzoides*: (H1) α-phellandrene-enriched fractions should show dose-dependent antinociceptive activity in a formalin or acetic-acid writhing assay, consistent with the mechanisms reported for the isolated compound; (H2) whole-extract and α-phellandrene-fraction anti-inflammatory activity should be reducible in a carrageenan-induced paw-oedema model. For *C. coelestinum*: (H3) hexadecanoic acid methyl ester- and phytol-enriched fractions should show antibacterial activity (disc-diffusion or broth microdilution MIC) against the Gram-positive pathogens implicated in the cited literature; (H4) whole-extract antioxidant capacity (DPPH or ORAC assay) should scale with phytol and hexadecanoic acid methyl ester content across the five localities, tracking the locality-level variation already documented in Table 5. None of these hypotheses is tested in the present manuscript; each is a specific, falsifiable prediction left as a defined next step, alongside the standard-compound co-injection and independent-material validation identified as priorities in Section 4.5.

4.7 Framework Positioning Relative to Existing Authentication Approaches

Table 8
and Table 9 consolidate the comparative and reproducibility points argued in Sections 4.1–4.2.

Approach	Species-level authentication	Chemical evidence	Pharmacological evidence
Classical morphological/anatomical taxonomy	Independent and foundational	Not used	Not addressed
Descriptive GC-MS profiling alone	Assumed, not re-verified at time of profiling	Compound list; no abundance/distribution classification	Frequently asserted without compound-level support
Conventional chemotaxonomy	Assumed from prior identification	Marker presence/absence across taxa	Not addressed
Literature-based phytochemical interpretation	Assumed	Not linked to specific authenticated markers	Narrative, unweighted, and often uncited to primary sources
DNA barcoding-based species authentication	Independent and molecular, but requires reference sequence databases that are sparse for many tropical taxa (Zhu et al., 2022)	Not addressed	Not addressed
Chromatographic fingerprint (HPTLC/HPLC) authentication	Assumed from prior identification	Whole-profile pattern matching, not marker-level classification	Not addressed
PADK (this framework)	Independently established first, before any chemical step (Phase 1)	Dual-axis classified and identification-confidence scored (Phase 2)	Criterion-based literature mining, equation-scored, and internally validated (Phases 3–5)

Table 8
Positioning of PADK relative to six adjacent authentication and profiling traditions used with medicinal plants, including molecular (DNA barcoding) and profile-matching (HPTLC/HPLC) approaches, to make explicit what PADK adds relative to each.

Component	Required input	Analytical step	Expected output
Botanical authentication	Field-collected voucher material; herbarium access	Morphological scoring; histological sectioning (Section 2.3)	Authenticated voucher identity, independent of chemistry (Table 1)
Chemotaxonomic authentication	GC-MS chromatograms (chloroform extract)	Dual-axis (abundance/distribution) marker classification; library-match confidence scoring (Section 2.4)	Classified marker inventory (Table 2)
Pharmacological annotation	Peer-reviewed literature databases (PubMed, ScienceDirect)	Criterion-based inclusion/exclusion search per marker (Section 2.5)	Annotation matrix with source-level evidence grade (Table 3)
Confidence scoring	Annotation matrix outputs	Weighted five-component equation, $CS = \Sigma W_i X_i$ (Section 2.6)	Star-rated confidence score per compound (Table 4)
Internal validation	Independent quantitative phytochemical dataset	Leave-one-locality-out nearest-centroid classification (Section 2.8)	Accuracy, sensitivity, specificity, confusion matrix (Table 5, Fig. 2)

Table 9. Reproducibility checklist summarizing the data inputs, analytical steps, and outputs required to re-apply PADK to a new species pair.

5. CONCLUSION

This paper tested whether species-level authentication of two morphologically convergent medicinal Asteraceae could be built from multiple independent evidence classes into one reproducible framework, rather than resting on any single line of evidence. We constructed, mathematically formalized, and

internally validated a five-phase framework, the Pharmacological Annotation Diagnostic Key (PADK), that authenticates species identity independently of chemistry, classifies chromatographic markers by abundance, distribution, and spectral identification confidence, mines and equation-scores the peer-reviewed pharmacological literature for each marker ($CS = \Sigma W_i X_i$), and compiles the result into a reproducible diagnostic key and a Therapeutic Signature Index (TSI = Σ(activity weight × compound confidence × relative abundance)). Applied to *Ageratum conyzoides* and *Conoclinium coelestinum*, the framework resolved two distinct, evidence-weighted chemotype signatures corroborated by leave-one-locality-out classification on out-of-sample phytochemical data (100% accuracy on a ten-sample held-out set), by convergence across three methodologically independent evidence classes, and, more loosely, by concordance with recorded ethnobotanical use. Every pharmacological statement in this manuscript remains a literature-derived annotation by design, not a demonstrated species property; Section 4.6 converts the confidence-ranked annotation matrix into four falsifiable experimental hypotheses that would close that gap. Because the five-phase structure does not depend on any feature specific to this genus pair or to volatile chemistry (Section 4.4), we offer PADK as a starting template for authenticating other taxonomically difficult medicinal species groups, while bounding, in Section 4.3, the conditions — a small validation sample chief among them — under which it should perform less well than it did here. PADK demonstrates feasibility and offers a transferable framework whose broader applicability remains to be tested, not a universally validated system; it gives plant systematists a way to stop treating morphological identity and pharmacological relevance as separately reported facts about a specimen, and start treating them as two tiers of one authenticated, evidence-traceable record.

Declarations

Competing interests:

The authors have no relevant financial or non-financial interests to disclose.

Ethical statement

This study involved plant material only; no human or animal subjects were used.

Funding:

This work was conducted as part of a self-funded doctoral research programme at the Department of Botany, Delta State University, Abraka, Nigeria.

Author Contribution

Ozioma Michael Emmanuel: Conceptualization, Methodology, Investigation, Data curation, Formal analysis, Validation, Visualization, Writing – original draft, Writing – review and editing, Project administration, Correspondence.Agbogidi, O.M.: Conceptualization, Methodology, Supervision, Validation, Writing – review and editing.Erhenhi, A. H. : Conceptualization, Methodology, Supervision, Validation, Writing – review and editing.

Acknowledgments:

The authors thank the Department of Botany, Delta State University, Abraka, for access to the DELSU Herbarium and Botanical Garden Site III used in specimen authentication.

Data availability:

Voucher specimens are deposited at the Delta State University Herbarium (DELSUH-309, DELSUH-269). Morphological, anatomical, quantitative phytochemical, and GC-MS datasets underlying Sections 3.1–3.8, including the full leave-one-locality-out validation data (Table 5), are available from the corresponding author on reasonable request.

References

1. Amin A, Park S (2025) Chemotaxonomy, an efficient tool for medicinal plant identification: current trends and limitations. Plants 14:2234. https://doi.org/10.3390/plants14142234
2. Betz JM, Brown PN, Roman MC (2011) Accuracy, precision, and reliability of chemical measurements in natural products research. Fitoterapia 82:44–52. https://doi.org/10.1016/j.fitote.2010.09.011
3. Gonçalves RLG, Cunha FVM, Sousa-Neto BPS, Oliveira LSA, Lopes ME, Rezende DC, Sousa IJO, Nogueira KM, Souza LKM, Medeiros JVR, Wong DVT, Pereira VMP, Lima-Júnior RCP, Sousa DP, Oliveira CPC, Almeida FRC, Oliveira FA (2020) α-Phellandrene attenuates tissular damage, oxidative stress, and TNF-α levels on acute model ifosfamide-induced hemorrhagic cystitis in mice. Naunyn Schmiedebergs Arch Pharmacol 393:1835–1848. https://doi.org/10.1007/s00210-020-01869-3
4. Heywood VH (2007) Taxonomy and plant conservation. BGjournal 4:12–15

5. Islam MT, Ali ES, Uddin SJ, Shaw S, Islam MA, Ahmed MI, Chandra Shill M, Karmakar UK, Yarla NS, Khan IN, Billah MM, Pieczynska MD, Zengin G, Malainer C, Nicoletti F, Gulei D, Berindan-Neagoe I, Apostolov A, Banach M, Yeung AWK, El-Demerdash A, Xiao J, Dey P, Yele S, Jóźwik A, Strzałkowska N, Marchewka J, Rengasamy KRR, Horbańczuk J, Kamal MA, Mubarak MS, Mishra SK, Shilpi JA, Atanasov AG (2018) Phytol: a review of biomedical activities. Food Chem Toxicol 121:82–94. https://doi.org/10.1016/j.fct.2018.08.032
6. Lima DF, Brandão MS, Moura JB, Leitão JMRS, Carvalho FAA, Miúra LMCV, Leite JRSA, Sousa DP, Almeida FRC (2012) Antinociceptive activity of the monoterpene α-phellandrene in rodents: possible mechanisms of action. J Pharm Pharmacol 64:283–292. https://doi.org/10.1111/j.2042-7158.2011.01401.x
7. Maltsev Y, Erst A (2023) Recent advances in the integrative taxonomy of plants. Plants 12:4097. https://doi.org/10.3390/plants12244097
8. Michael OE, Agbogidi OM, Erhenhi AH (2026) Taxonomic profiling of Ageratum conyzoides L. and Conoclinium coelestinum (L.) DC.: homologous species from tropical genera of Asteraceae. PhD thesis, Delta State University, Abraka
9. Page MJ, McKenzie JE, Bossuyt PM, Boutron I, Hoffmann TC, Mulrow CD, Shamseer L, Tetzlaff JM, Akl EA, Brennan SE, Chou R, Glanville J, Grimshaw JM, Hróbjartsson A, Lalu MM, Li T, Loder EW, Mayo-Wilson E, McDonald S, McGuinness LA, Stewart LA, Thomas J, Tricco AC, Welch VA, Whiting P, Moher D (2021) The PRISMA 2020 statement: an updated guideline for reporting systematic reviews. BMJ 372:n71. https://doi.org/10.1136/bmj.n71
10. Patterson TF, Nesom GL (2006) Conoclinium. In: Flora of North America Editorial Committee (eds) Flora of North America north of Mexico, vol 21. Oxford University Press, New York, pp 477–479
11. Shaaban MT, Ghaly MF, Fahmi SM (2021) Antibacterial activities of hexadecanoic acid methyl ester and green-synthesized silver nanoparticles against multidrug-resistant bacteria. J Basic Microbiol 61:557–568. https://doi.org/10.1002/jobm.202100061
12. Simpson MG (2010) Plant systematics, 2nd edn. Academic Press, Amsterdam
13. Siqueira HDS, Neto BS, Sousa DP, Gomes BS, da Silva FV, Cunha FVM, Wanderley CWS, Pinheiro G, Cândido AGF, Wong DVT, Ribeiro RA, Lima-Júnior RCP, Oliveira FA (2016) α-Phellandrene, a cyclic monoterpene, attenuates inflammatory response through neutrophil migration inhibition and mast cell degranulation. Life Sci 160:27–33. https://doi.org/10.1016/j.lfs.2016.07.008
14. Sundar RDV, Arunachalam S (2025) 2,4-Di-tert-butylphenol from endophytic fungi Fusarium oxysporum attenuates the growth of multidrug-resistant pathogens. Front Microbiol 16:1575021. https://doi.org/10.3389/fmicb.2025.1575021
15. Tibshirani R, Hastie T, Narasimhan B, Chu G (2002) Diagnosis of multiple cancer types by shrunken centroids of gene expression. Proc Natl Acad Sci USA 99:6567–6572. https://doi.org/10.1073/pnas.082099299
16. Zhu S, Liu Q, Qiu S, Dai J, Gao X (2022) DNA barcoding: an efficient technology to authenticate plant species of traditional Chinese medicine and recent advances. Chin Med 17:112. https://doi.org/10.1186/s13020-022-00655-y

Figures

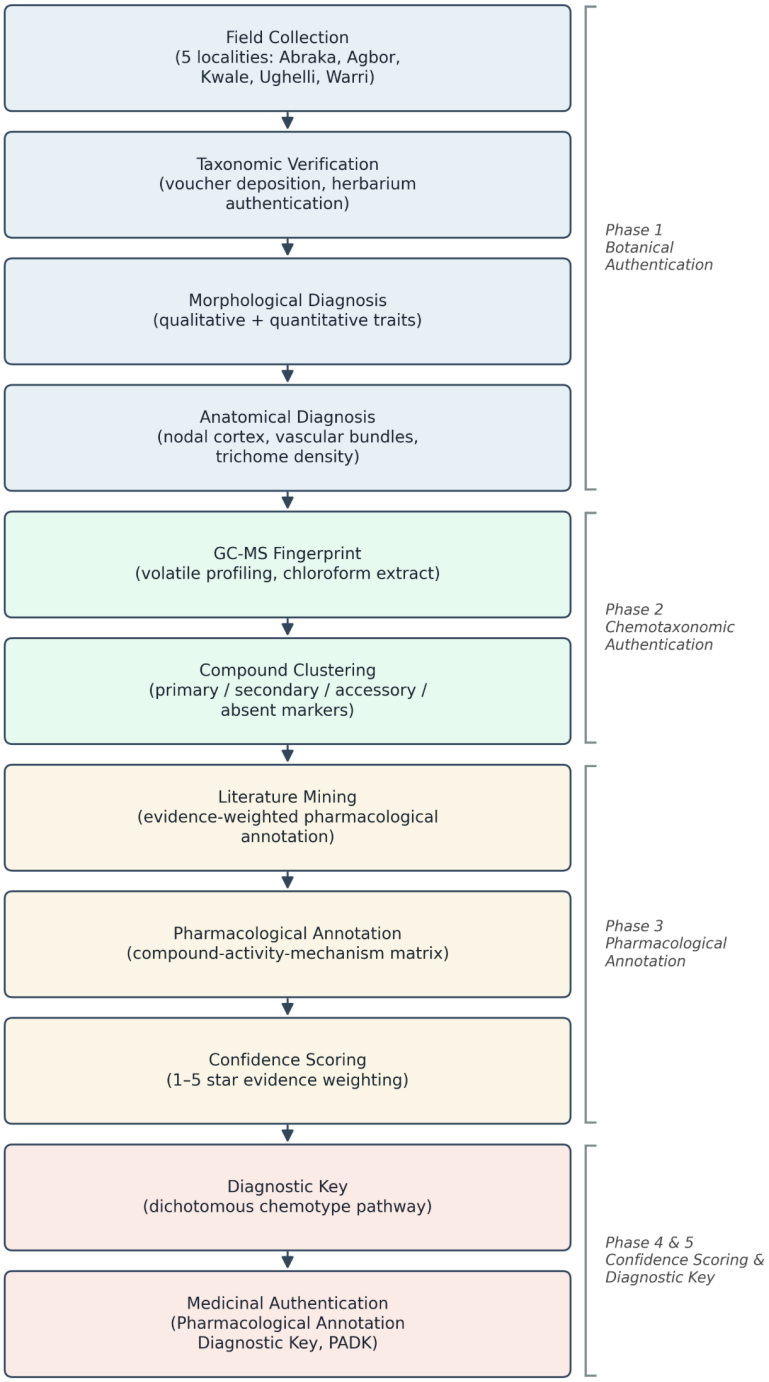

Figure 1

The five-phase Pharmacological Annotation Diagnostic Key (PADK) construction pipeline, from field collection to medicinal authentication.

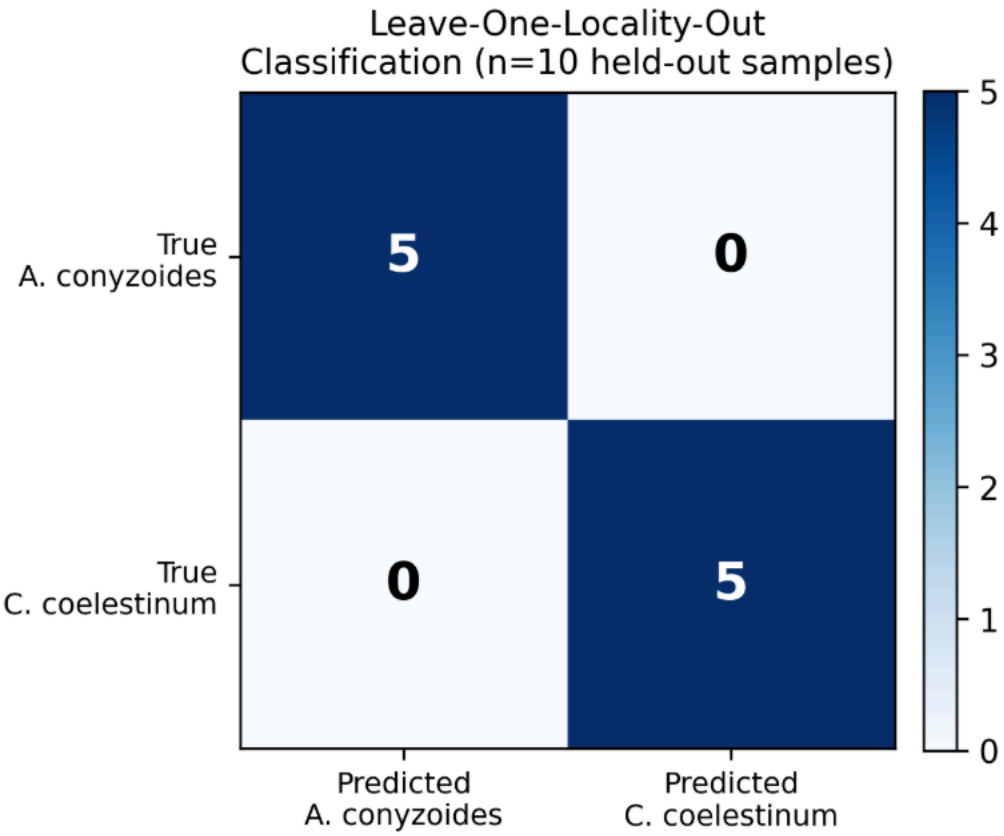

Figure 2

Confusion matrix for leave-one-locality-out classification (accuracy = 100%, n = 10 held-out samples; sensitivity = specificity = precision = 100%).

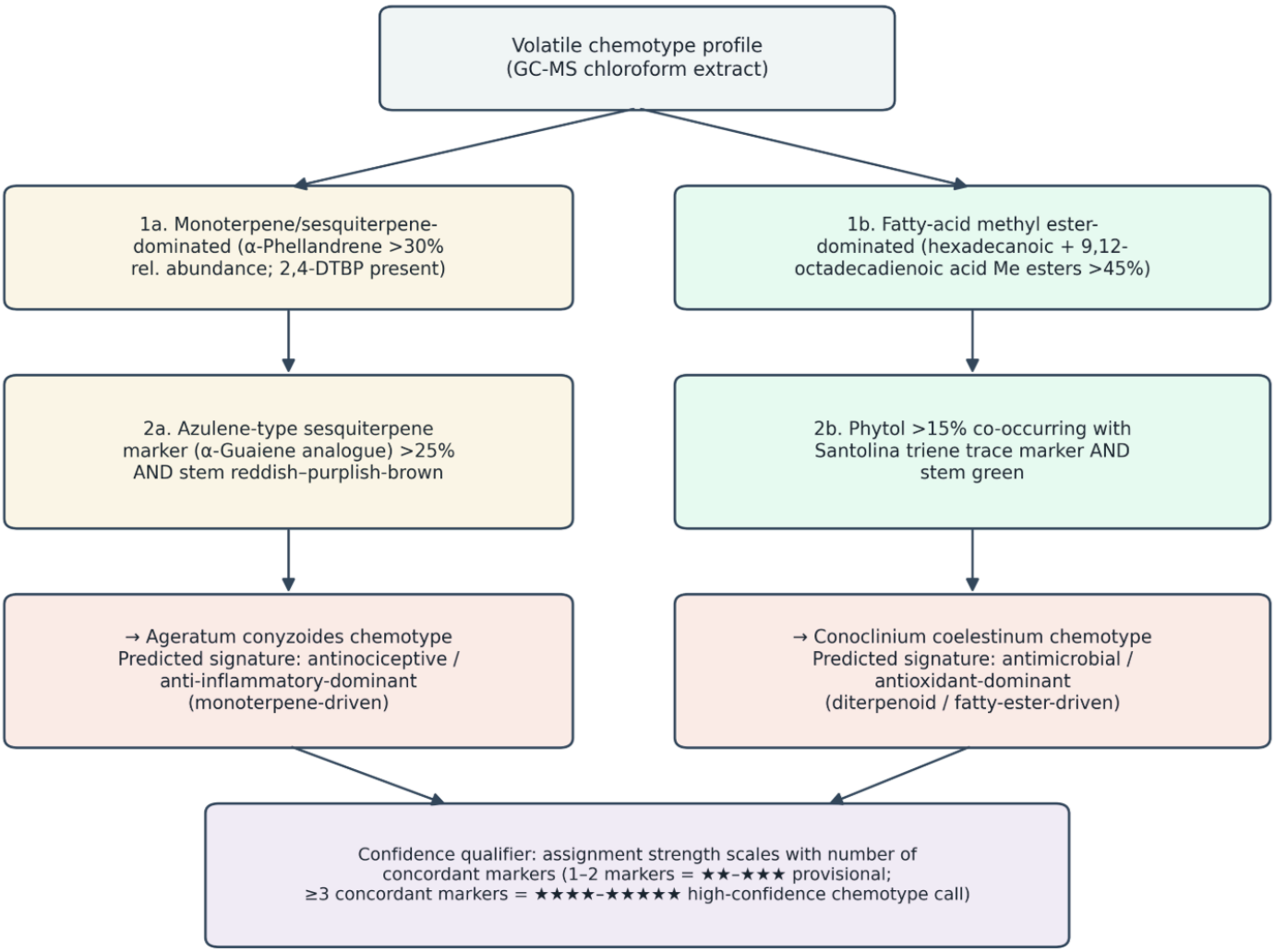

Figure 3

Dichotomous Pharmacological Annotation Diagnostic Key (PADK) routing GC-MS chemotype markers, cross-checked against Phase 1 morphology, to a species-level call and predicted therapeutic signature.

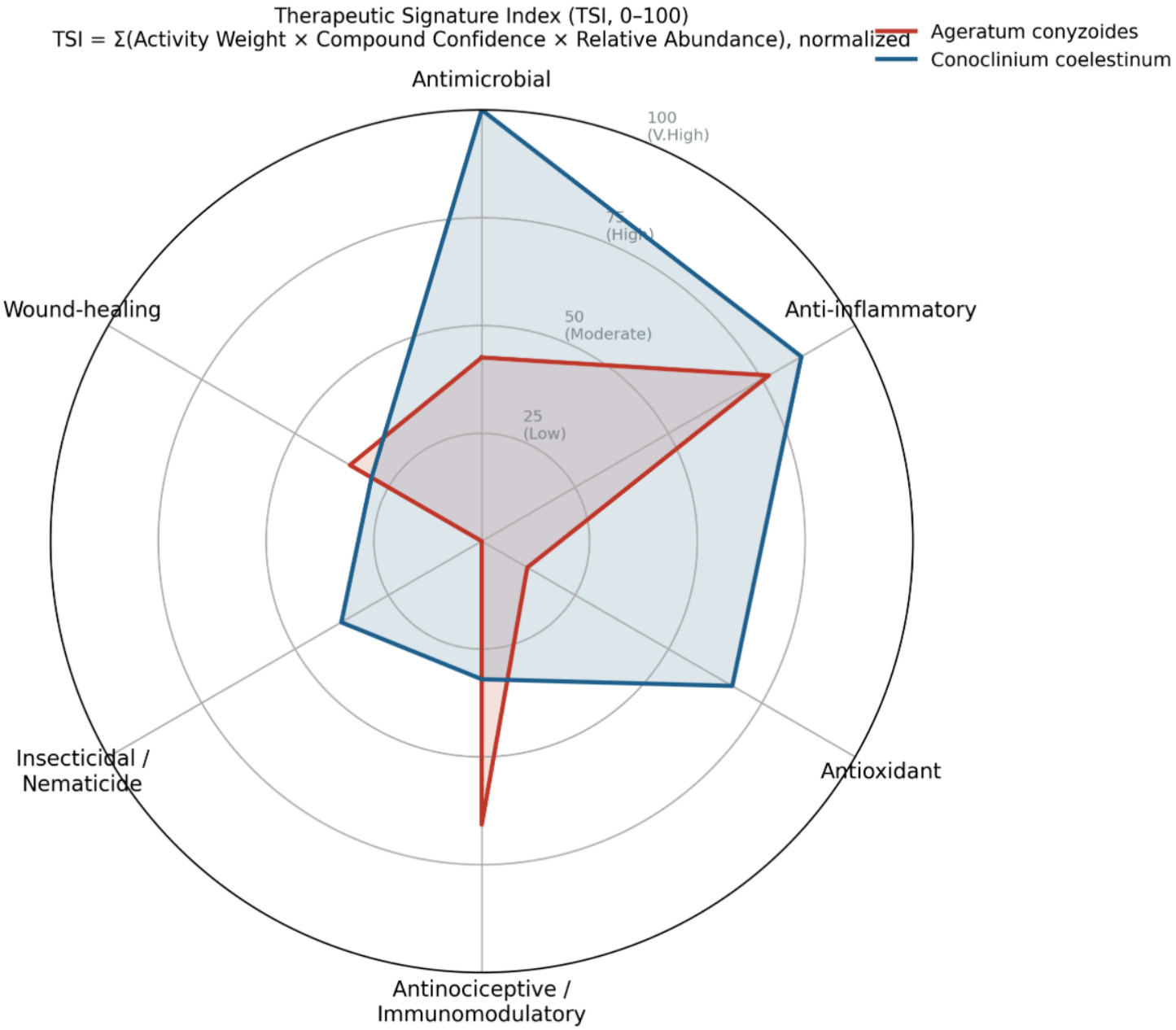

Figure 4

Therapeutic Signature Index (TSI, 0–100, normalized) comparing *Ageratum conyzoides* and *Conoclinium coelestinum* across six pharmacological axes. TSI(s) = Σ[w × CS × Abund(s)], normalized to the matrix maximum.